Supporting Information for

Two-Dimensional PdSn Meso-Macroporous Nanosieves for Robust Methanol Electrooxidation

Xiyue Zhang,[a] Wen Zhang,[a] Fei Gao,[a] Chang Zhou,[a] Tienan Zhang,[a] Yunchong Cao,[a] Shanshan Zhang,[a] Tingjie Mao,[b] Juan Wang,[b]* and Yangping Zhang,[a]**

[a] School of Environmental and Chemical Engineering, Jiangsu University of Science and Technology, Zhenjiang, 212003, China

[b] College of Chemistry and Materials Engineering, Wenzhou University, Wenzhou, 325035, China

*Corresponding author: E-mail: gaofei006@just.edu.cn (F. Gao),

juanwang@wzu.edu.cn (J. Wang), ypzhang@just.edu.cn (Y. Zhang).

Experimental Section

1. Reagents and chemicals

Sodium tetrachloropalladate ($NaPdCl_4$, ≥98%), Tin(II) oxalate (C_2O_4Sn, ≥99.7%), hexacarbonyl tungsten ($W(CO)_6$, ≥97%) was purchased from Energy Chemical Co., Ltd. (Shanghai, China). N, N-Dimethylformamide (DMF, ≥99.5%), methanol (CH_4O, ≥99.5%), acetic acid ($C_2H_4O_2$, ≥99%) were purchased from Sinopharm Chemical Reagent Co. Ltd. (Shanghai, China). All chemicals were used without any purifications. The water (18 MΩ cm^{-1}) used in all experiments was obtained by passing through an ultrapure purification system.

2. Synthesis of sub-two nanometer Pd_4Sn Meso-Macroporous Nanosieves (MNSs), Pd_2Sn MNSs and Pd_8Sn MNSs.

For the synthesis of Pd_4Sn MNSs, typically, $NaPdCl_4$ (10 mg), C_2O_4Sn (1.5 mg), $W(CO)_6$ (30mg) was dispersed in 2 mL acetic acid and 8 mL DMF with ultrasonication. Then, the mixture was heated in an oil bath at 140 °C for 3h. The products were collected by centrifugation and washed with ethanol for 3 times, then disperse in ethanol for further use. The synthesis of Pd_2Sn MNSs and Pd_8Sn MNSs was similar to

that of Pd_4Sn MNSs by simply alter the content of C_2O_4Sn.

3. Characterizations

The morphologies, sizes, and structures of the catalysts were observed using transmission electron microscopy (TEM, acceleration voltage: 120 kV, HT-7700), and high-resolution transmission electron microscopy (HRTEM, working voltage: 200 kV, F20). X-ray diffraction (XRD) spectra were collected by the X'Pert-Pro MPD diffractometer (Netherlands PANalytical) with a 40 kV Cu Kα radiation. The contents of Pd and Sn were determined by scanning electron microscopy-energy dispersive X-ray spectroscopy (SEM-EDS) with a working voltage of 15 kV. X-ray photoelectron spectroscopy (XPS) was performed on a VG Scientific ESCALab 220 XL spectrometer using 300 W Al Kα radiation to identify the valence states and chemical bonds of various elements in the samples.

4. Electrochemical measurements

The tests were carried out on a CHI660E electrochemical workstation manufactured by Shanghai Chenhua Instrument Co., Ltd., China. A three-electrode system was employed (counter electrode: a platinum wire; reference electrode: a saturated calomel electrode (SCE); working electrode: a glassy-carbon electrode (GCE) with a diameter of 5 mm). Before tests, GCE was polished with aluminum oxide (Al_2O_3) until its surface became shiny. As for the working electrode preparation, 2 mg of different catalysts were ultrasonically dispersed in a mixture containing 496 μl of isopropanol and 4 μl of Nafion (5%) for 30 minutes to form a homogeneous catalyst ink. Initially, 5 μL of the catalyst ink was dropped onto the surface of the polished GCE and allowed to dry. Subsequently, another 3 μL of the ink was dropped to ensure the catalyst completely covered the working electrode, and then it was dried again. The cyclic voltammetry (CV) curves in 0.5 M KOH at a scan rate of 50 mV s^{-1} were recorded to measure the electrochemical active surface area (ECSA) value. The MOR tests were operated in 0.5 M KOH and 1 M methanol. The catalytic stability was evaluated by chronoamperometry (i-t) tests and successive CV tests. For comparison, commercial Pd/C (JM, 20 wt% Pd) was used as the as the control catalyst.

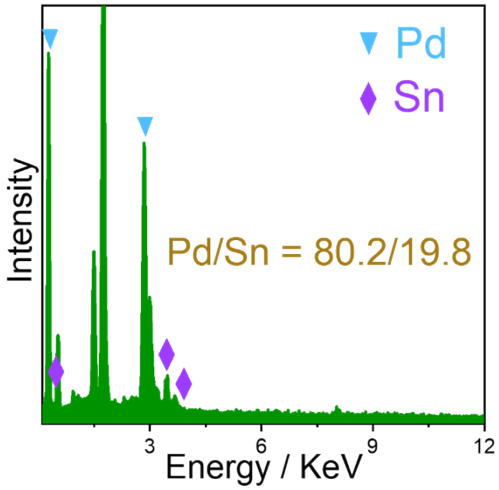

Fig. S1 EDS pattern of Pd_4Sn MNSs.

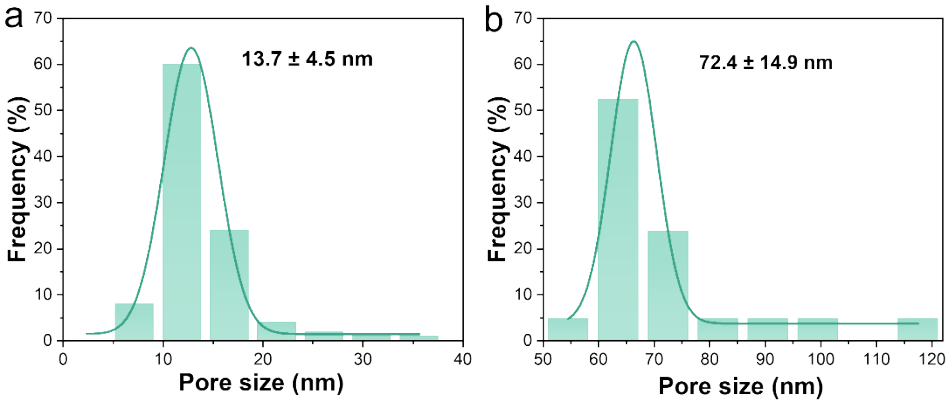

Fig. S2 Pore size distribution histograms of Pd_4Sn MNSs for (a) mesopores and (b) macropores.

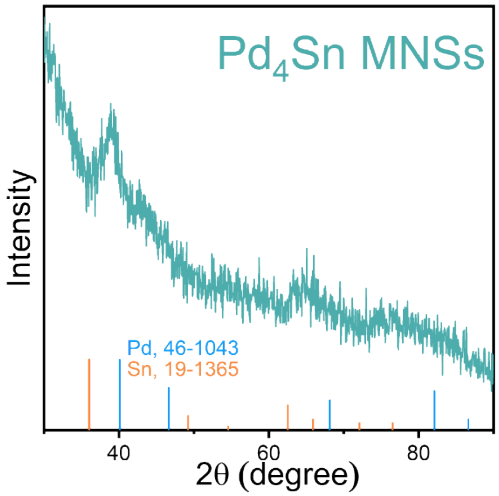

Fig. S3 XRD pattern of Pd_4Sn MNSs.

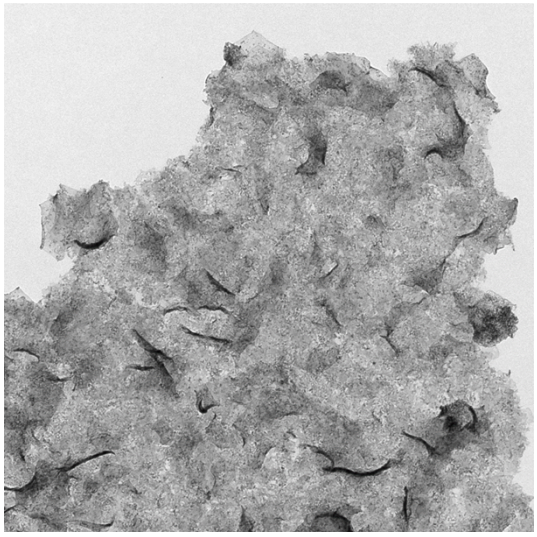

Fig. S4 Additional TEM images of Pd_2Sn MNSs.

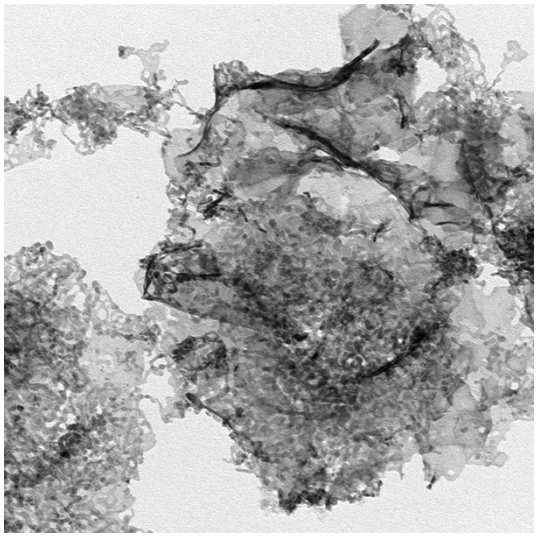

Fig. S5 Additional TEM images of Pd_8Sn MNSs.

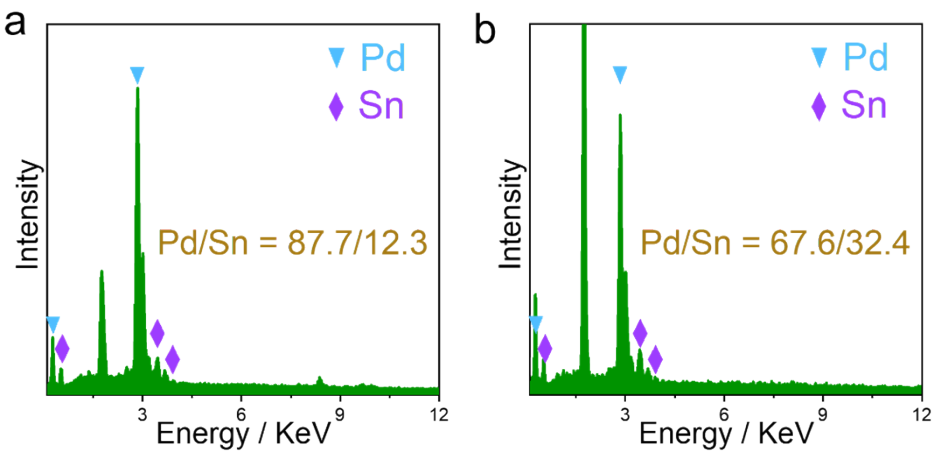

Fig. S6 EDS pattern of (a) Pd_8Sn MNSs and (b) Pd_2Sn MNSs.

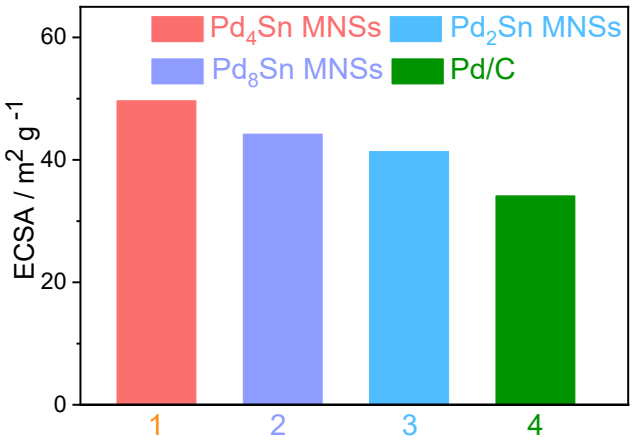

Fig. S7 Calculated ECSA values of Pd_4Sn MNSs, Pd_8Sn MNSs, Pd_2Sn MNSs and Pd/C catalysts, respectively.

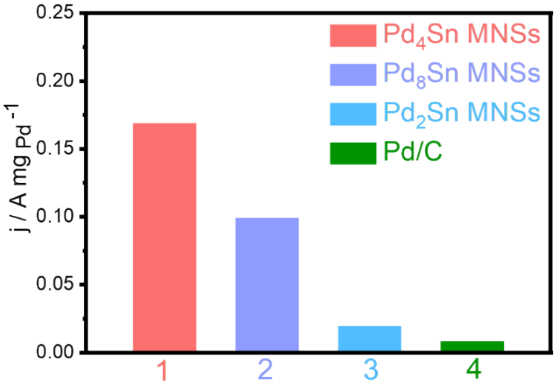

Fig. S8 Calculated remaining activity of Pd_4Sn MNSs, Pd_8Sn MNSs, Pd_2Sn MNSs and Pd/C catalysts after i-t tests.

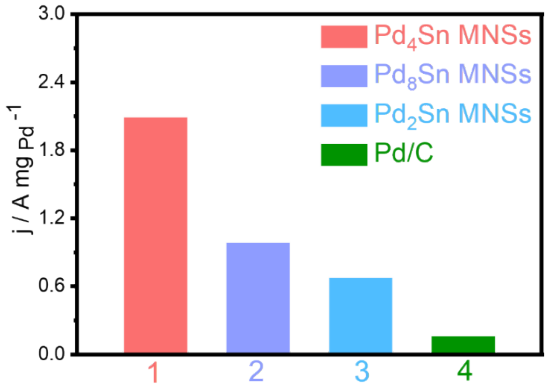

Fig. S9 Calculated remaining activity of Pd_4Sn MNSs, Pd_8Sn MNSs, Pd_2Sn MNSs and Pd/C catalysts after 500 successive cycles.

The reaction evolution processes of MOR[1, 2].

$*CH_3OH \rightarrow *CH_2OH + H^+ + e^-$ (1)

$*CH_2OH \rightarrow *CHOH + H^+ + e^-$ (2)

$*CHOH \rightarrow *CHO + H^+ + e^-$ (3)

$*CHO + H_2O \rightarrow *HCOOH + H^+ + e^-$ (4-1)

$*CHO \rightarrow *CO + H^+ + e^-$ (4-2)

$*HCOOH \rightarrow *COOH + H^+ + e^-$ (5-1)

$*CO + H_2O \rightarrow *COOH + H^+ + e^-$ (5-2)

$*COOH \rightarrow *CO_2 + H^+ + e^-$ (6)

The symbol * represents the catalyst. Among them, equations (4-1) and (5-1) represent the non-CO pathway of the MOR, while equations (4-2) and (5-2) correspond to the CO pathway. The other reaction steps are identical in both the CO and non-CO pathways.

1. Y. Qin, K. Yu, G. Wang, Z. Zhuang, Y. Dou, D. Wang and Z. Chen, *Angew. Chem. Int. Ed.*, 2025, **64**, e202420817.

2. Y. Lv, P. Liu, R. Xue, Q. Guo, J. Ye, D. Gao, G. Jiang, S. Zhao, L. Xie, Y. Ren, P. Zhang, Y. Wang and Y. Qin, *Adv. Sci.*, 2024, **11**, e2309813.

Table. S1 MOR performances of Pd_4Sn MNSs and various electrocatalysts from published works.

Catalysts	Peak currents from CV curves		Electrolyte	Reference
	J_m (A mg^{-1})	J_s (mA cm^{-2})		
Pd_4Sn MNSs	2.321	4.67	0.5 M KOH + 1 M CH_3OH	This work
Pd_4Sn WNWs	1.04	0.12	0.1 M KOH + 0.5 M CH_3OH	*Nano Lett.,* **2019**, 19, 6894-6903
CrO_X-Pd	2.05	5.30	1 M KOH + 1 M CH_3OH	*Nano Lett.,* **2023**, 23, 9555-9562
Pd-PdO PNTs	1.111	4.69	0.1 M KOH + 0.3 M CH_3OH	*Adv. Funct. Mater.,* **2020**, 30, 2000534.
$Pd_{72}Cu_{14}Co_{14}$	1.062		1 M KOH + 1 M CH_3OH	*J. Energy Chem.,* **2019**, 29, 72.
Pd-Co J-NWs	1.205	3.584	1 M KOH + 1 M CH_3OH	*ACS Appl. Mater. Inter.,* **2018**, 10, 29965
PdAg@Pd	1.38	1.50	0.5 M NaOH + 1 M CH_3OH	*J. Power Sources,* **2018**, 398, 201.
PdFe NCs	1.07	3.4	1 M KOH + 1 M CH_3OH	*Nanoscale*, **2020**, 12, 2126–2132.
Pd_2Cu_2/rGO	0.916		1 M KOH + 1 M CH_3OH	*J. Mater. Sci.,* **2018**, 53, 15871.
$Pd_{0.52}Ag$	1.38		0.5 M NaOH + 1 M CH_3OH	*Angew. Chem. Int. Ed.,* **2019**, 58, 8794-8798